Diamond & Related Materials 64 (2016) 8–12

Contents lists available at ScienceDirect

Diamond & Related Materials

journal homepage: www.elsevier.com/locate/diamond

Charge transfer dynamics in poly(3-hexylthiophene): nanodiamond blend films

Wei-Long Xu, Fei Zheng, Xiao-Yu Yang, Han-Dong Jin, Lin Feng, Xiao-Tao Hao *

School of Physics and State Key Laboratory of Crystal Materials, Shandong University, Jinan, Shandong 250100, China

ARTICLE INFO

Article history:
Received 24 November 2015
Received in revised form 4 January 2016
Accepted 4 January 2016
Available online 7 January 2016

Keywords:
Nanodiamond
Charge transfer
Conjugation length
Morphology

ABSTRACT

The introduction of nanodiamond (ND) into regioregular poly(3-hexylthiophene) (P3HT) can vary the conformational structure of the polymer. The microstructure of the blend films was analyzed by various techniques, such as absorption spectra, Raman spectra and X-ray diffraction. It is shown that the presence of ND improves the crystallinity and increases the effective conjugation length of P3HT in the blend films. Furthermore, the photo-excited dynamics between P3HT and ND were studied by the steady-state and time-resolved photoluminescence techniques. An obvious fluorescence quenching in the blend films demonstrates the high efficiency of photoinduced charge transfer between P3HT and ND. The energy transfer dynamics could be excluded owing to the bandgap of ND is larger than P3HT. The morphology of the blend films was investigated by Kelvin probe force microscope and transmission electron microscopy. The interpenetrating network of P3HT fibrils and ND domains facilitates charge transfer between the two materials, resulting in the obvious fluorescence quenching of the polymer. The enhanced photocurrent in a prototypical device based on P3HT:ND blends may be correlated with the high efficiency of charge transfer from P3HT to ND.

© 2016 Elsevier B.V. All rights reserved.

1. Introduction

Over the past decades, organic solar cells (OSCs) based on conjugated polymers have attracted considerable attention because of their advantageous properties including flexibility, low weight and roll-to-roll production [1]. To date, best-performance OSCs with power conversion efficiency beyond 10% can only be achieved using a specific electron-acceptor material fullerene [2,3]. Fullerene works particularly for OSCs, because of the near-ball shape structure which facilitates forming three dimensional charge transfer network. In addition, the small domain size and high electron mobility of fullerene are also responsible for the high performance of the OSCs [4]. Despite the high performance, fullerene undergoes some drawbacks such as poor photostability, difficulty in synthesis and high production cost [5,6]. Therefore, non-fullerene acceptor materials have been explored as potential alternatives to replace fullerene such as PbS, TiO_2 and ZnO nanocrystals [7–10]. Besides, novel carbon-based materials including carbon nanotubes, graphene and graphite oxides have emerged as the acceptors for OSCs, owing to the tunable optical and electronic properties [11–14]. Ren et al. [11] achieved high efficiency of hybrid solar cells via utilization of semiconductor single-walled carbon nanotube. Stylianakis et al. [12] fabricated poly(3-hexylthiophene) (P3HT): graphite oxide bulk heterojunction solar cells, yielding a power conversion efficiency enhancement of 2 orders of magnitude compared with that of pristine P3HT. Liu et al. [13] used graphene as the acceptor material and achieved 1.4% efficiency in the OSC. Besides, graphene could also be used in P3HT:PCBM system to balance the carrier mobility [14]. Recently, some innovative electron acceptors are challenging fullerene with high power conversion efficiency reaching 5.5%–6.8% [4–6].

Carbon-based semiconductor nanodiamond (ND) is intriguing to modify the properties in polymer composites [15–17]. ND particles have a few advantages, for instance, abundant in nature, easily surface functionalized, non-toxic and high chemical and physical stability [18, 19]. Lau et al. [16] reported 53% photocurrent increment in P3HT:PCBM bulk heterojunction solar cells by adding small amount of nanodiamond as the charge transporter. At the same time, Hsiao et al. [15] investigated the size effect of ND on the performance of P3HT:PCBM solar cells. Besides, the incorporation of small quantity of ND into P3HT film could enhance the photoconductivity of P3HT significantly [17].

In the work, the impact of ND on the conjugation length and the crystalline structure of P3HT films was investigated with absorption spectra, Raman spectra and X-ray diffraction (XRD) methods. Steady-state and time-resolved photoluminescence (PL) techniques were applied to study the photo-excited dynamics of the P3HT:ND blend films. The morphology and phase separation in P3HT:ND blend films were explored by Kelvin probe force microscope (KPFM) and transmission electron microscope (TEM). Finally, the relationship between current and voltage (I–V) under illumination of a prototypical device was investigated to further explore the charge transfer dynamics between P3HT and ND.

* Corresponding author.
E-mail address: haoxt@sdu.edu.cn (X.-T. Hao).

http://dx.doi.org/10.1016/j.diamond.2016.01.003
0925-9635/© 2016 Elsevier B.V. All rights reserved.

2. Experimental section

P3HT and ND were purchased from Sigma-Aldrich and PlasmaChem respectively and used as received without further purification. The diameter of ND is less than 5 nm. P3HT solution was prepared in chloroform at a concentration of 5 mg ml^{-1} and mixed with ND at a weight ratio of 1:x, where x is the weight ratio of P3HT to ND, ranging from 10 wt.% to 50 wt.%. The uniform films were obtained by spin-coating method at a rotation speed of 1200 rpm for 60 s.

Optical absorption spectra were recorded in the transmission mode by using a UV–Vis spectrophotometer (TU-1900, PG Instruments, Ltd) with two light beams. One is the reference light, and the other one was used to monitor the absorption change. Raman spectra were measured by a confocal Raman microscope (LabRam HR800). XRD measurements were performed using a PANalytical Empyrean diffractometer. The steady-state PL spectra were obtained using a fiber optic spectrometer (PG2000 Pro, Idea Optics Co., Ltd.) with an excitation wavelength of 400 nm. Time-resolved PL decay kinetics were measured by fluorescence upconversion technique. The excitation light was generated from frequency doubling a femtosecond Ti-sapphire laser (Maitai HP, Spectra-Physics) at 80 MHz. The emission from example was mixed with the "gate" beam in a nonlinear crystal for sum frequency generation. The upconverted photons were passed through a monochromator and detected with a photon counting photomultiplier tube. The magnitude of the upconverted signal was detected as a function of delay between the excitation and gate pulses. The surface morphology and potential are measured by a KPFM (Solver P47 PRO, NTMDT Co.). TEM studies were conducted with a JEM-100CX II TEM (JEOL).

The prototypical devices were fabricated with a sandwich structure of glass/ITO/active layer/Al. The blend solutions were spin-coated with a rotation speed of 1200 rpm for 60 s to form films serving as active layer. Al was deposited by thermal evaporation in vacuum with a base pressure of $<1.0 \times 10^{-4}$ Pa at an evaporation rate of 0.3 Å/s. The performance of the devices was measured under AM1.5G illumination of 100 mW/cm^2 provided by a solar simulator (Sofn Instruments Co., Ltd. China). The I–V curves of the devices were obtained by a programmable voltage–current sourcemeter (2400, Keithley Instruments Inc., Cleveland, OH, USA).

3. Results and discussion

Conformational structure of conjugated polymers can be revealed by steady-state absorption spectra [17]. Absorption spectra of P3HT and P3HT:ND blend films are shown in Fig. 1a. The absorption spectrum of P3HT shows one peak at 518 nm and two shoulders at 558 nm and 605 nm. A clear red-shift occurs in the P3HT absorption spectrum with ND addition. Besides, the enhanced intensity of 605 nm shoulder can be observed with the content of ND increment. Kim et al. [20] pointed out that the vibronic feature at 605 nm demonstrates a high degree of ordered crystalline lamellae in P3HT film due to strong interchain interaction. This indicates that the effective conjugation of P3HT is increased upon ND addition. The Raman data were also obtained to better understand the effect of ND on the molecular structure of P3HT. The inset in Fig. 1b shows the Raman scattering of P3HT with a wide scattering region ranging from 900 to 1900 cm^{-1}. There are various Raman modes: the main in-plane ring skeleton modes at 1450 cm^{-1} (symmetric CC stretch mode) and at 1384 cm^{-1} (C—C intraring stretch mode), the inter-ring C—C stretch mode at 1208 cm^{-1}, the C—H bending mode with the C—C inter-ring stretch mode at 1190 cm^{-1} [21]. Among these modes, the emphases were focused on the two main in-plane ring skeleton modes at 1450 and 1384 cm^{-1}, as they are considered to be sensitive to π-electron delocalization of P3HT molecules [21], and at the same time the characteristic peaks of ND do not occur at the two positions [19]. The positions of in-plane CC and C—C peaks of P3HT are almost constant with ND addition. Nevertheless, the full width at half maximum (fwhm) of the two main peaks are decreased with the ND addition, as shown in Fig. 1b. This implies better molecular order of P3HT in the P3HT:ND blend films [22]. Solution-processed conjugated P3HT thin films demonstrate semi-crystalline structure with ordered microcrystalline domains embedded in an amorphous matrix [23]. The XRD spectra shown in Fig. 1c indicate the peak position centered at $2\theta = 5.2^{\circ}$ derives from (100) reflection of P3HT-crystallites with *a*-axis orientation [24]. The intensity of (100) peak in P3HT film is relatively weak compared with that in previous works, which may be related to the different preparation process [23]. The P3HT:ND composite films showed similar XRD patterns but with stronger and narrower peak compared with that in pristine P3HT film. The crystalline level of P3HT can be calculated according to the Debye–Scherer relationship: $L = 0.9\lambda/(\Delta 2\theta)\cos\theta$, where L is the coherence length, $\lambda = 1.54$ Å, the peak position is located at $2\theta = 5.2^{\circ}$ and $\Delta 2\theta$ is fwhm of the scattering peak. The narrower peak of (100) reflection with ND content increment illustrates that the crystallinity of P3HT was improved in the blend films. The crystalline lengths were 9.3 nm, 10.2 nm, 10.6 nm and 10.8 nm in P3HT, with 10 wt.% ND addition, 20 wt.% ND addition and 50 wt.% ND addition respectively, as shown in Fig. 1d. The increased crystallinity of P3HT after ND addition may be due to the diffusion of nanoparticle molecules to nucleation sites forming hexagonal aggregation [17]. Therefore, the combination of absorption spectra, Raman spectra and XRD validate that the addition of ND into P3HT is beneficial to increase the conjugation length and improve the crystallinity of P3HT.

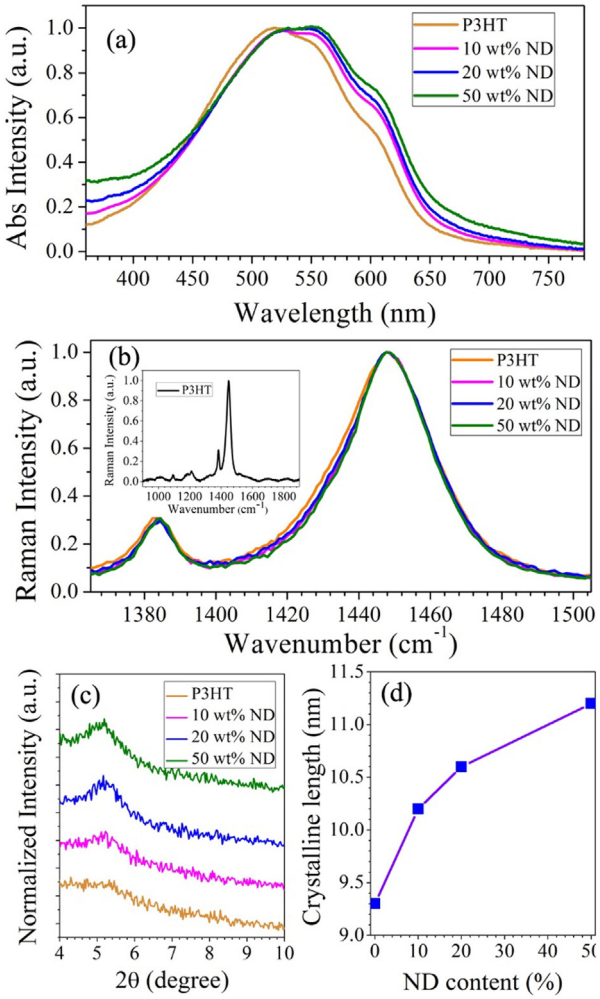

Fig. 1. (a–d) Absorption spectra, Raman spectra, XRD pattern and crystalline length of P3HT and P3HT:ND blend films with different ND content respectively. A wide Raman absorption spectra of P3HT film is demonstrated in the inset of (b).

In order to understand the photo-excited dynamics between P3HT and ND, steady-state and time-resolved PL spectra were performed on

Download English Version:

https://daneshyari.com/en/article/7111261

Download Persian Version:

https://daneshyari.com/article/7111261

Daneshyari.com